Non-Hermitian quantum system generated from two coupled Sachdev-Ye-Kitaev models

Wenhe Cai[1], Sizheng Cao,[1] Xian-Hui Ge,[1,*] Masataka Matsumoto[1], and Sang-Jin Sin[2,†]

[1]*Department of Physics, Shanghai University, Shanghai, 200444, China*
[2]*Department of Physics, Hanyang University, Seoul 04763, Korea*

We show that a non-Hermitian two coupled Sachdev-Ye-Kitaev (SYK) model can provide thermodynamic structure equivalent to a Hermitian two coupled SYK model. The energy spectrum, the entanglement degree of the ground states and the low energy effective action of this model are not influenced by the non-Hermiticity. The novel biorthogonal ground states demonstrates that two SYK sites, one of which can be in the ground state and the other in the Schwarzian excited state by tuning the non-Hermiticity. We find evidence that the free energy is independent of the non-Hermiticity.

I. INTRODUCTION

Recently, non-Hermitian physics has gained widespread attention, such as non-Hermitian linear response theory [1], non-Hermitian topological systems [2,3] and non-Hermitian holography [4,5]. One of the primary reasons for those studies is due to the probability in nature effectively becomes nonconserving due to the presence of energy, particles, and information regarding the external degrees of freedom that are out of the Hilbert space. In a non-Hermitian system experiencing an exceptional point in the wave momentum, the corresponding eigenfrequencies change from real to complex numbers [6–10]. However, seminal work by Bender and Boettcher demonstrates that in the physics of non-Hermitian systems, a huge class of nonconservative Hamiltonians can exhibit entirely real spectra as long as they commute with the parity-time (PT) operator [11]. Moreover, all the PT symmetric Hamiltonians studied reported in the literature exhibited such property [12–14]. The similarity transformations can also enable one to construct a non-Hermitian Hamiltonian with real spectrum [14–16].

In a quantum many-body system, the quantum two-level system can be simulated by coupling two copies of the Sachdev-Ye-Kitaev (SYK) model. The SYK mode, which is well-known as a disordered and strongly-coupled quantum system composed of Majorana fermions [17–19], has recently emerged as an exemplary model providing insight into the nature of non-Fermi liquids [20], quantum chaos [21], holography [22,23], strange metallic transport [24,25] and high temperature superconducting [26,27]. The SYK model is closely related to two-dimensional dilaton gravity describing excitations above the near horizon external black hole [28,29]. Therefore, an eternal traversable wormhole can be constructed by considering two copies of SYK models coupled by a simple interaction. This Maldacena-Qi (MQ) model demonstrates that at low temperature, the coupling can drive phase transitions to a phase holographically dual to an eternal traversable wormhole with an AdS$_2$ throat [30]. Conversely, at a higher temperature, the system reduces to two gapless black hole phases [30]. However, in the non-Hermitian setup, one may expect this gapped-gapless physical picture drastically changed.

The main goal of this paper is to prove that the wormhole-black hole picture is robust not only in a Hermitian two coupled SYK model, but also in a non-Hermitian two coupled SYK model. For this purpose, we propose a novel non-Hermitian two-site SYK model. We first prove that the system yields real energy spectrum. Furthermore, we show that the degree of entanglement, the low energy effective action and the phase structure are non-Hermiticity independent. As illustrated in Fig. 1, even though these two SYK sites are approaching a "ground state/excited state" picture in the regime of strong non-Hermitian limit, the thermodynamic phase structure indicates three distinct properties at different temperatures.

II. NON-HERMITIAN TWO COUPLED SYK MODEL

We consider a non-Hermitian two coupled SYK model with the Hamiltonians

*gexh@shu.edu.cn
†sjsin@hanyang.ac.kr
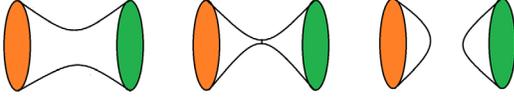
FIG. 1.   Sketched phase diagram for the physical picture. Left: a geometry connecting the two sides in the low temperature regime. The left Sachdev-Ye-Kitaev (SYK) and right SYK are in different states because of the non-Hermitian parameter. Middle: an unstable geometry connecting two SYK sites. Right: two separated SYK sites at high temperature represent the gapless two black hole phases. The non-Hermitian parameter can change the states of the left and right SYK sites, which are marked in orange and green colors. When $\alpha = 0$, the phase diagram recovers that of [30].

$$H = -\sum_{ijkl}^{N} J_{ijkl} \sum_{A=R,L} (c_1 C_i^{A\dagger} C_j^{A\dagger} C_k^A C_l^A$$
$$+ c_2 C_i^{A\dagger} C_j^A C_k^{A\dagger} C_l^A) + H_{\text{int}},$$
$$H_{\text{int}} = i\mu \sum_i^N (e^{-2\alpha} C_i^{L\dagger} C_i^R - e^{2\alpha} C_i^{R\dagger} C_i^L), \qquad (1)$$

where $A = L$, R refers to the "left" and "right" side of the two identical copies, and c_1 and c_2 are two real valued constants. We choose $c_1 = 2$ and $c_2 = 4$ in what follows to match to the MQ model [30]. Note that other choices of positive c_1 and c_2 do not change the total physical picture. The parameter α is a real number controlling the strength of non-Hermiticity, which is introduced by a non-Hermitian particle-hole similarity transformation (see Appendix A for details). Under the self-similarity transformation, Dirac fermions C and $C^\dagger$ are introduced to replace the Majorana fermions ψ in the MQ model. The coupling J_{ijkl} are random real numbers, which obey the Gaussian distribution and satisfy $J_{ijkl} = -J_{jikl} = -J_{ijlk} = J_{klij}$ with $\langle J_{ijkl} \rangle = 0$, $\langle J_{ijkl}^2 \rangle = \frac{J^2}{8N^3}$. For this reason, we call this model a pseudo-complex SYK to distinguish from the usual complex SYK. By analytically continued to an imaginary value $\alpha \to i\alpha$, one can recover the Hermitian Hamiltonian.

III. ENERGY SPECTRUM AND DEGREE OF ENTANGLEMENT

The energy spectrum is an important feature of the non-Hermitian quantum system. We compute the energy spectrum by using exact diagonalization techniques. The energy spectrum is real and independent of the non-Hermitian parameter α, as demonstrated in Fig. 2.

For non-Hermitian systems, we need to construct the ground state by introducing a biorthogonal set $\{|\psi_n^l\rangle, |\psi_n^r\rangle\}$ [14–16,31]. The right/left eigenstates are defined as

$$H|\psi_n^r\rangle = E_n|\psi_n^r\rangle, H^\dagger|\psi_m^l\rangle = E_m^*|\psi_m^l\rangle. \qquad (2)$$

The eigenstates satisfy the properties as follows:
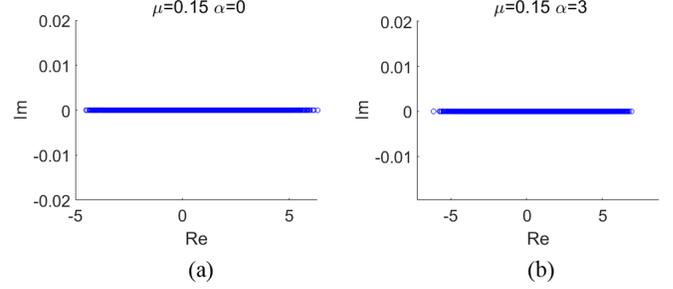
FIG. 2.   Plots of the spectrum with $\mu = 0.15$, $N = 8$ for the values of $\alpha = 0$ (a) and for the values of $\alpha = 3$ (b).

$$\sum_n |\psi_n^l\rangle\langle\psi_n^r| = I, \langle\psi_n^l|\psi_m^r\rangle = \delta_{nm}. \qquad (3)$$

We impose the constraints that system yields the ground state energy as those of [32] by taking $H_{\text{int}}^\dagger|\psi_0^l\rangle = -\mu N|\psi_0^l\rangle$, $H_{\text{int}}|\psi_0^r\rangle = -\mu N|\psi_0^r\rangle$ and $\langle\psi_0^l|\psi_0^r\rangle = 1$. Without loss of generality, the generated ground states are proposed as

$$|\psi_0^r\rangle = \prod_j^N (\tilde{A}|1\rangle_{L,j}|0\rangle_{R,j} + i\tilde{B}|0\rangle_{L,j}|1\rangle_{R,j}), \qquad (4)$$

$$|\psi_0^l\rangle = \prod_j^N (\tilde{C}|1\rangle_{L,j}|0\rangle_{R,j} + i\tilde{D}|0\rangle_{L,j}|1\rangle_{R,j}), \qquad (5)$$

where the coefficients $\tilde{A}$, $\tilde{B}$, $\tilde{C}$ and $\tilde{D}$ satisfy the relation $\tilde{B} = \tilde{A}e^{2\alpha}$ and $\tilde{D} = \tilde{C}e^{-2\alpha}$. The constraint $\langle\psi_0^l|\psi_0^r\rangle = 1$ further leads to $\tilde{A}\tilde{C} = \tilde{B}\tilde{D} = \frac{1}{2}$. The ground states can return to the ground state of the Hermitian case ($\alpha = 0$) consistently if setting

$$\tilde{A} = \frac{1}{\sqrt{2}}, \qquad \tilde{B} = \frac{e^{2\alpha}}{\sqrt{2}}, \qquad \tilde{C} = \frac{1}{\sqrt{2}}, \qquad \tilde{D} = \frac{e^{-2\alpha}}{\sqrt{2}}. \qquad (6)$$

In the biorthogonal set, the usual orthogonal normalization is not applicable.

In our non-Hermitian model, the degree of entanglement turns out to be

$$P_E = -\text{tr}(\rho_A \log \rho_A) = 1, \qquad (7)$$

which can be derived from the von-Neumann entropy of the reduced density matrix,

$$\rho_{LR} = |\psi_0^r\rangle\langle\psi_0^l| = \tilde{A}\tilde{C}|10\rangle\langle01| + i\tilde{B}\tilde{C}|01\rangle\langle01|$$
$$- i\tilde{A}\tilde{D}|10\rangle\langle10| + \tilde{B}\tilde{D}|01\rangle\langle10|). \qquad (8)$$

$$\rho_L = \text{tr}_R(\rho_{LR}) = \begin{pmatrix} \tilde{A}\tilde{C} & 0 \\ 0 & \tilde{B}\tilde{D} \end{pmatrix}. \qquad (9)$$

Because of $P_E = 1$, which is independent of α, the ground states are maximally entangled between two systems.

The ground states (4) and (5) will approach the pure state for large α, but the degree of entanglement remains unchanged. Taking the limit $\alpha \to -\infty$, we have

$$|\psi_0^r\rangle \to \prod_j^N \frac{1}{\sqrt{2}}|1\rangle_{L,j}|0\rangle_{R,j}, \quad |\psi_0^l\rangle \to \prod_j^N \frac{ie^{-2\alpha}}{\sqrt{2}}|0\rangle_{L,j}|1\rangle_{R,j},$$

$$(10)$$

while in the limit $\alpha \to +\infty$, we obtain

$$|\psi_0^l\rangle \to \prod_j^N \frac{i}{\sqrt{2}}|0\rangle_{L,j}|1\rangle_{R,j}, \quad |\psi_0^r\rangle \to \prod_j^N \frac{ie^{2\alpha}}{\sqrt{2}}|0\rangle_{L,j}|1\rangle_{R,j}.$$

$$(11)$$

Therefore, the left and right SYK sites are no longer symmetric as illustrated in Fig. 1.

IV. LOW ENERGY EFFECTIVE ACTION

In order to see the effects of the non-Hermitian parameter, we study low energy properties of both in the extended SYK model and the gravity description. In the low energy limit, the model simplifies due to the emergence of a conformal symmetry. The retarded Green's function of the non-Hermitian system is defined as

$$G_{AB}(\tau_1, \tau_2) = \frac{1}{N}\sum_n \langle\psi_n^l|T C_i^{A\dagger}(\tau_1) C_i^B(\tau_2)|\psi_n^r\rangle, \quad (12)$$

where $A, B = L, R$. The saddle-point equations are invariant under the time reparametrization $\tau \to h(\tau)$ and the $U(1)$ symmetry, which is the same as the complex SYK model in [33–36]:

$$\tilde{G}_{AB}(\tau_1, \tau_2) = [h_A'(\tau_1)h_B'(\tau_2)]^\Delta G_{AB}(h(\tau_1), h(\tau_2))$$
$$e^{i\phi_A(\tau_1)-i\phi_B(\tau_2)},$$

$$\tilde{\Sigma}_{AB}(\tau_1, \tau_2) = [h_A'(\tau_1)h_B'(\tau_2)]^{1-\Delta}\Sigma_{AB}(h(\tau_1), h(\tau_2))$$
$$e^{i\phi_B(\tau_2)-i\phi_A(\tau_1)}.$$

In the absence of the interacting term, the Schwarzian effective action of the left or right copy turns out to be

$$S_A = -N\alpha_S \int d\tau \left\{\tanh\frac{h_A(\tau)}{2}, \tau\right\}$$
$$+ \frac{NK}{2}\int d\tau (\phi_A'(\tau) + i\varepsilon_A h_A'(\tau))^2, \quad (13)$$

where ε_A is related to the $U(1)$ charge Q_A and α_S is determined by four-point calculation of the SYK model. The above effective action is given by the Schwarzian derivative,

$$\{h, \tau\} = \frac{h'''(\tau)}{h'(\tau)} - \frac{3}{2}\left(\frac{h''(\tau)}{h'(\tau)}\right)^2.$$

The effective action of the coupled part is written as

$$S_{\text{int}} = \frac{\mu}{2}\int d\tau \left[\frac{bh_L'(\tau)h_R'(\tau)}{\cosh^2\frac{h_L(\tau)-h_R(\tau)}{2}}\right]^\Delta \cosh(\varepsilon h_L(\tau) - \varepsilon h_R(\tau))$$
$$\times [e^{i(\phi_L-\phi_R)-2\alpha} + e^{-i(\phi_L-\phi_R)+2\alpha}]. \quad (14)$$

This action has the global $SL(2) \times U(1)$ symmetry generated by

$$\delta h_L = \epsilon^0 + \epsilon^+ e^{ih_L} + \epsilon^- e^{-ih_L},$$
$$\delta h_R = \epsilon^0 - \epsilon^+ e^{ih_R} - \epsilon^- e^{-ih_R},$$
$$\delta\phi_A = -i\varepsilon\delta h_A + \epsilon, \quad (15)$$

where $\varepsilon_L = \varepsilon_R = \varepsilon$.

The total action could be simplified to

$$\frac{S}{N} = -2\alpha_S \int d\tau \left\{\tanh\frac{h(\tau)}{2}, \tau\right\} + K\int d\tau(\phi'(\tau) + i\varepsilon h'(\tau))^2$$
$$+ \frac{\mu}{2^{2(\Delta-1)}}\int d\tau(h'(\tau))^{2\Delta}, \quad (16)$$

with the solution

$$h_L = h_R = h(\tau), \qquad \phi_L = \phi_R - 2i\alpha = \phi(\tau), \quad (17)$$

where we have chosen $b^\Delta = N$. In Appendix B, we derive the $SL(2)$ Noether charges. The $SL(2)$ Noether charge vanishes with the simple solution $h(\tau) = t'\tau$, so it can be treated as gauge symmetry. The solutions of Eq. (17) lead to $Q_\pm = 0$, and

$$Q_0/N = 2e^{-\phi}[-\phi'' - e^{2\phi} + \Delta\mu e^{2\Delta\phi}] = 0, \quad (18)$$

by introducing $\phi = \log h'$. We can derive the equations of motion from the action of a nonrelativistic particle in a potential

$$S = N\int du[(\phi')^2 - (e^{2\phi} - \mu e^{\phi/2})]. \quad (19)$$

The effective potential is independent of the non-Hermitian parameter α, but the same as that of the MQ model [30]. One can therefore conclude that there is an α-independent energy gap at low energy.

We can thus add a boundary interaction to the bulk action

$$S_{\text{int}} = g\sum_{i=1}^N \int du(e^{-2\alpha}O_L^{i\dagger}(u)O_R^i(u) - e^{2\alpha}O_R^{i\dagger}(u)O_L^i(u)), \quad (20)$$

where O is a set of N operators with dimension Δ and g is proportional to the coupling μ. When α and g are small, the interacting term in Eq. (20) corresponds to the interaction term of the low energy effective action in Eq. (14). The coupling of left and right black holes $(1 - 2\alpha)O_L^{i\dagger}O_R^i$, $(1 + 2\alpha)O_R^{i\dagger}O_L^i$ are not symmetric. The two sides of AdS$_2$ are

directly coupled by the double trace deformation. Since $e^{2\alpha}$ or $e^{-2\alpha}$ is always positive, the double trace interaction generates negative null energy in the bulk without violating causality the same as that of [37]. Therefore quantum entangled states at left and right boundaries are connected.

V. THERMODYNAMIC PHASE STRUCTURE BEYOND THE LOW ENERGY LIMIT

At finite temperature, the retarded Green's function receives a great contribution from the non-Hermitian parameter α. But the whole thermodynamic phase structure remains unchanged as the non-Hermitian parameter α varies.

The effective action can be obtained as

$$
\frac{S_{\text{eff}}}{N} = -\log \det(\sigma_{AB} - \Sigma_{AB})
$$
$$
- \int d\tau_1 d\tau_2 \bigg(\Sigma_{BA}(\tau_2, \tau_1) G_{AB}(\tau_1, \tau_2)
$$
$$
+ \frac{36}{4} J^2 G_{AB}^2(\tau_1, \tau_2) G_{BA}^2(\tau_2, \tau_1) \bigg), \quad (21)
$$

where

$$
\sigma_{AB} = \begin{pmatrix} \partial_\tau & i\mu e^{-2\alpha} \\ -i\mu e^{2\alpha} & \partial_\tau \end{pmatrix}. \quad (22)
$$

The corresponding equations can be written as

(a)

(b)

(c)

(d)
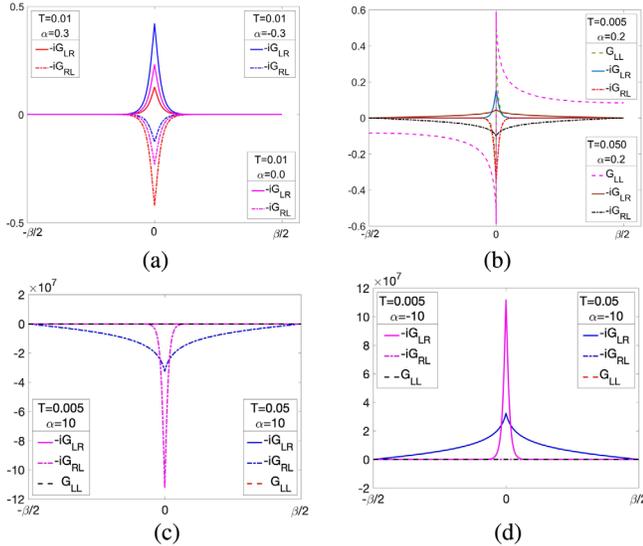
FIG. 3. (a) Green's function with $\alpha = 0, \pm 0.3$ at temperature $T = 0.01$. (b) Green's function with $\alpha = 0.2$ at low temperature $T = 0.005$ or high temperature $T = 0.05$. (c) Green's function with $\alpha = 10$ at low temperature $T = 0.005$ or high temperature $T = 0.05$. (d) Green's function with $\alpha = -10$ at low temperature $T = 0.005$ or high temperature $T = 0.05$.

$$
\Sigma_{AB}(\tau_1, \tau_2) = -36J^2 G_{AB}^2(\tau_1, \tau_2) G_{BA}(\tau_2, \tau_1),
$$
$$
G_{LL}(i\omega_n, \alpha) = \frac{-i\omega_n - \Sigma_{LL}(i\omega_n, \alpha)}{D(i\omega_n, \alpha)},
$$
$$
G_{RR}(i\omega_n, \alpha) = \frac{-i\omega_n - \Sigma_{RR}(i\omega_n, \alpha)}{D(i\omega_n, \alpha)},
$$
$$
G_{LR}(i\omega_n, \alpha) = \frac{-i\mu e^{-2\alpha} + \Sigma_{LR}(i\omega_n, \alpha)}{D(i\omega_n, \alpha)},
$$
$$
G_{RL}(i\omega_n, \alpha) = \frac{i\mu e^{2\alpha} + \Sigma_{RL}(i\omega_n, \alpha)}{D(i\omega_n, \alpha)},
$$
$$
D(i\omega_n, \alpha) = (-i\omega_n - \Sigma_{LL})(-i\omega_n - \Sigma_{RR})
$$
$$
+ (i\mu e^{-2\alpha} - \Sigma_{LR})(i\mu e^{2\alpha} + \Sigma_{RL}), \quad (23)
$$

with the Matsubara frequency $\omega_n = 2\pi(n + \frac{1}{2})/\beta$. The numerical results in Fig. 3(a) show that $G_{RR}(i\omega_n, \alpha) = G_{LL}(i\omega_n, \alpha)$, $G_{LR}(i\omega_n, \alpha) = -G_{RL}(i\omega_n, -\alpha)$. When $\alpha = 0$, the model recovers the pseudo-complex SYK model at zero chemical potential [32]. Green's function decays exponentially,

$$
G_{ab}(\tau) \sim e^{-E_{gap}\tau} \quad (24)
$$

(see Appendix C for details) within a certain α region at low temperature, and the correlators decay as a power law like SYK behavior at high temperatures, as shown in Fig. 3(b). The Green's functions can be considered as the order parameter. When α is large enough, the off-diagonal Green's function decays exponentially no matter at low temperature $T = 0.005$ or high temperature $T = 0.05$, and E_{gap} decreases as temperature increases from $T = 0.005$ to $T = 0.05$ [see Figs. 3(c) and 3(d)]. According to the approximate behavior of the saddle-point equations [Eq. (23)], as $\alpha \to +\infty$, the off-diagonal Green's function $G_{RL} \sim -\frac{1}{\Sigma_{LR}}$ dominates while as $\alpha \to -\infty$, the term $G_{LR} \sim -\frac{1}{\Sigma_{RL}}$ dominates. The approximate solutions are indicative of decoupled SYK behavior in the IR limit ($G \sim -\frac{1}{\Sigma}$). The results with $\alpha = 10$ support this statement numerically in Figs. 3(c) and 3(d).

We evaluate the free energy of this non-Hermitian coupled model in this section. Substituting the saddle-point solutions into the action in Eq. (21) as the method in [38], we obtain the free energy

$$
\frac{F}{N} = -T \frac{\log Z}{N} = T \frac{S_{\text{eff}}}{N}
$$
$$
= -T \bigg[2\log 2 + \sum_{\omega_n} \log \frac{D(i\omega_n, \alpha)}{(i\omega_n)^2}
$$
$$
+ \sum_{\omega_n} \bigg(\frac{3}{4}\Sigma_{LL}(i\omega_n, \alpha)G_{LL}(i\omega_n, \alpha) + \frac{3}{4}\Sigma_{RR}(i\omega_n, \alpha)
$$
$$
\times G_{RR}(i\omega_n, \alpha) + \frac{3}{4}\Sigma_{LR}(i\omega_n, \alpha)G_{RL}(i\omega_n, \alpha)
$$
$$
+ \frac{3}{4}\Sigma_{RL}(i\omega_n, \alpha)G_{LR}(i\omega_n, \alpha) \bigg) \bigg]. \quad (25)
$$
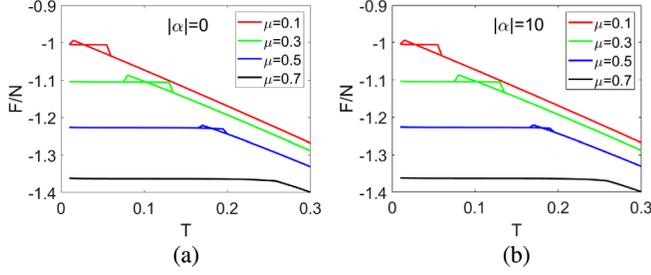
FIG. 4. The free energy as a function of T with different coupling μ for the values of $|\alpha| = 0, 10$ and $J = 1/6$. Starting from the high temperature, we decrease the temperature to low value, and then increase it again back to the high temperature value.

The free energy as a function of temperature is plotted in Fig. 4. The free energy obtained in Fig. 4 is analogous to the free energy of the pseudo-complex SYK model with the Hermitian coupled term in Refs. [32,39,40]. The first-order phase transition from the low temperature traversable wormhole phase to the high temperature two black hole phase ends at a second-order critical point ($T_c = 0.25$, $\mu_c = 0.7$), which is not influenced by the non-Hermitian parameter.

VI. CONCLUSION AND DISCUSSION

We have constructed a novel non-Hermitian two coupled SYK model yielding a real energy spectrum. This is a pseudo-Hermitian Hamiltonian, where the non-Hermiticity is reflected in the coupling between two copies of the pseudo-complex SYK model. The ground states of the total Hamiltonian receive a contribution from the non-Hermitian parameter. In the strong non-Hermitian limit, the wave function $|\psi_0^r\rangle$ approaches the "ground states" on the left and "excited states" on the right or vice versa. The effective action and the free energy are α independence, although the left and right side states are actually α dependent. To understand this, let us analyze the non-Hermitian parameter dependence of the free energy. As mentioned previously, only $G_{LR} \sim -\frac{1}{\Sigma_{RL}}$ exists in Eq. (25) when $\alpha \to -\infty$, and only $G_{RL} \sim -\frac{1}{\Sigma_{LR}}$ exists in Eq. (25) when $\alpha \to +\infty$. Since Green's function and the self-energy satisfy $\Sigma_{LR}(i\omega_n, \alpha) = -\Sigma_{RL}(i\omega_n, -\alpha)$, the free energy does not change in the limit $\alpha = \pm\infty$ obviously. Low energy analysis further reveals an α-independent energy gap. However, a key observation is that the off-diagonal Green's functions G_{LR} and G_{RL} are no longer symmetric and strongly α dependent. Note that the transmission amplitude of particles across the traversable wormhole is proportional to the retarded Green's function. Thus, this may elucidate the observable aspects of the dynamics.

ACKNOWLEDGMENTS

APPENDIX A: NON-HERMITIAN SIMILARITY TRANSFORMATION

In this section, we provide more details about a similarity transformation on the left-hand side and the right-hand side Majorana fermion. One can generalize the phase ϕ from a real number to an imaginary number $\phi = -i\alpha$ and the imaginary phase transformation becomes a non-Hermitian particle-hole similarity transformation $C \to e^{\pm\alpha}C$ and $C^\dagger \to e^{\pm\alpha}C^\dagger$. It can be written as

$$\psi_{2i-1}^L = e^\alpha C_i^L + e^{-\alpha} C_i^{L\dagger}, \quad \psi_{2i}^L = i(e^\alpha C_i^L - e^{-\alpha} C_i^{L\dagger})$$
$$\psi_{2i-1}^R = e^{-\alpha} C_i^R + e^\alpha C_i^{R\dagger}, \quad \psi_{2i}^R = i(e^{-\alpha} C_i^R - e^\alpha C_i^{R\dagger}). \quad \text{(A1)}$$

After the self-similarity transformation, the Majorana fermions become non-Hermitian $(\psi^L)^\dagger \neq (\psi^L)$, $(\psi^R)^\dagger \neq \psi^R$ as long as $\alpha \neq 0$ in which the fermions $C^L, C^R, C^{L\dagger}, C^{R\dagger}$ satisfy the anticommutation relations as follows:

$$\{C_i^{A\dagger}, C_j^B\} = \delta_{ij}\delta_{AB}, \qquad \{C_i^{A\dagger}, C_j^{B\dagger}\} = \{C_i^A, C_j^B\} = 0.$$

We consider the ψ_{2i-1} case for simplicity of our calculation. In principle, the parameter α could be introduced by performing the non-Hermitian particle-hole similarity transformation on the MQ model,

$$H = -\sum_{ijkl}^N J_{ijkl}(\psi_{2i-1}^L \psi_{2j-1}^L \psi_{2k-1}^L \psi_{2l-1}^L$$
$$+ \psi_{2i-1}^R \psi_{2j-1}^R \psi_{2k-1}^R \psi_{2l-1}^R) + i\mu \sum_i \psi_{2i-1}^L \psi_{2i-1}^R. \quad \text{(A2)}$$

Note that all the nonphysical terms should be dropped out after the similarity transformation. So the Hamiltonian of the $\alpha = 0$ case is not exactly that of the MQ model.

APPENDIX B: NOETHER CHARGE

In this section, we discuss the Noether charges associated with the $SL(2)$ symmetry in the low energy effective action. The action is given by the combination of (13) and (14) in the main text. The general form of the Noether charge is described by

$$Q = \sum_{k\geq 1}^N \left(\frac{d}{d\tau}\right)^{k-1} \left[Y \sum_{m\geq k}^N \binom{m}{k} \left(-\frac{d}{d\tau}\right)^{m-k} \frac{\partial L}{\partial h^{(m)}}\right], \quad \text{(B1)}$$

where the infinitesimal transformation is given by $\tau \to \tau + aY$ with a small parameter a. Since the effective

Lagrangian contains up to third-derivative terms, the Noether charge can be explicitly written as

$$Q = Y\left[\frac{\partial L}{\partial h'} - \left(\frac{\partial L}{\partial h''}\right)' + \left(\frac{\partial L}{\partial h'''}\right)''\right]$$
$$+ \frac{dY}{d\tau}\left[\frac{\partial L}{\partial h''} - 3\left(\frac{\partial L}{\partial h'''}\right)'\right] + \frac{d^2Y}{d\tau^2}\left(\frac{\partial L}{\partial h'''}\right). \quad (B2)$$

Considering the $SL(2)$ transformation generated by (15) in the main text, the corresponding charges are given by

$$\frac{Q_0}{N} = Q_0[h_L, \phi_L] + Q_0[h_R, \phi_R] + \left(\frac{1}{h'_L} + \frac{1}{h'_R}\right)I_c, \quad (B3)$$

$$\frac{Q_+}{N} = Q_+[h_L, \phi_L] - Q_+[h_R, \phi_R] + \left(\frac{e^{ih_L}}{h'_L} - \frac{e^{ih_R}}{h'_R}\right)I_c, \quad (B4)$$

$$\frac{Q_-}{N} = Q_-[h_L, \phi_L] - Q_-[h_R, \phi_R] + \left(\frac{e^{-ih_L}}{h'_L} - \frac{e^{-ih_R}}{h'_R}\right)I_c, \quad (B5)$$

where

$$Q_0[h, \phi] = i\varepsilon K(\phi' + i\varepsilon h') - \alpha_S\left(h' + \frac{h'''}{h'^2} - \frac{h''^2}{h'^3}\right), \quad (B6)$$

$$Q_+[h, \phi] = e^{ih}\left[i\varepsilon K(\phi' + i\varepsilon h') - \alpha_S\left(-\frac{h''}{h'} + \frac{h'''}{h'^2} - \frac{h''^2}{h'^3}\right)\right], \quad (B7)$$

$$Q_-[h, \phi] = e^{-ih}\left[i\varepsilon K(\phi' + i\varepsilon h') - \alpha_S\left(\frac{h''}{h'} + \frac{h'''}{h'^2} - \frac{h''^2}{h'^3}\right)\right], \quad (B8)$$

$$I_c = \mu\Delta\left[\frac{bh'_L h'_R}{\cosh^2\frac{h_L - h_R}{2}}\right]^{\Delta}\cosh(\varepsilon h_L - \varepsilon h_R)$$
$$\times \cosh(2\alpha - i\phi_L + i\phi_R). \quad (B9)$$

Therefore, the zero charge conditions $Q_+ = Q_- = 0$ are satisfied if we set $h_L = h_R$. In addition, we study the constraint on the relation between ϕ_L and ϕ_R by considering the invariance of the effective action under the transformation of h_a and ϕ_a [40]. Then, we require

$$0 = \delta\sum_A (\phi'_A + i\varepsilon h'_A)^2$$
$$= 2\sum_A (\delta\phi'_A + i\varepsilon\delta h'_A)(\phi'_A + i\varepsilon h'_A), \quad (B10)$$
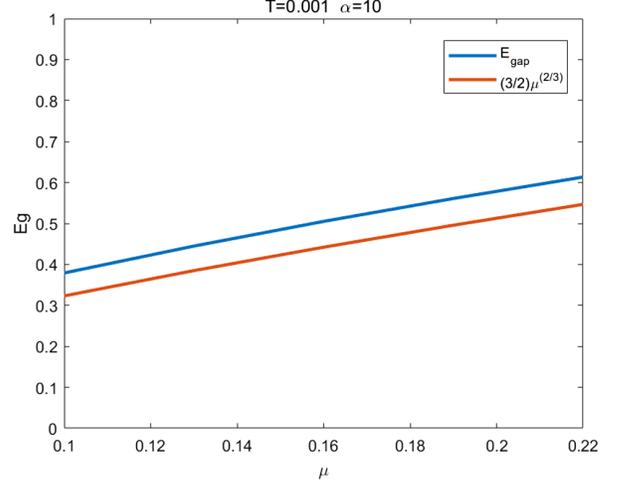
FIG. 5. The energy gap extracted from the exponential decay at low temperature $T = 0.001$ with $\alpha = 10$. The red line represents the power law behavior $E_{gap} \sim \mu^{2/3}$.

and

$$0 = \delta\cosh(2\alpha - i\phi_L + i\phi_R)$$
$$= \sinh(2\alpha - i\phi_L + i\phi_R)\delta(\phi_L - \phi_R), \quad (B11)$$

where we have assumed $h_L = h_R$. These conditions are satisfied if $\phi_L = \phi_R - 2i\alpha$ and $\delta\phi_L = -\delta\phi_R = \epsilon(\tau)$, where ϕ_L and ϕ_R are constants and $\epsilon(\tau)$ is an arbitrary infinitesimal function. To be self-consistent, the Noether charge associated with the variation of $\delta\phi_L = -\delta\phi_R = \epsilon(\tau)$ is given by

$$Q_\phi/N = K[(\phi'_L - \phi'_R) + i\varepsilon(h'_L - h'_R)], \quad (B12)$$

which vanishes if $h_L = h_R$ and $\phi_L = \phi_R - 2i\alpha$.

APPENDIX C: ENERGY GAP

As mentioned in the main text, the Green function decays exponentially $G_{ab}(\tau) \sim e^{-E_{gap}\tau}$. In Fig. 5, we show that the energy gap extracted from the exponential decay of $G_{AB}(\tau)$ in which the gap scaling $E_{gap} \sim \mu^{2/3}$, same as that of the Hermitian two coupled SYK model in [30]. The gap scaling in Fig. 5 indicates that our non-Hermitian model returns to the Hermitian model consistently if setting $\alpha = 0$.

[1] L. Pan, X. Chen, Y. Chen, and H. Zhai, Non-Hermitian linear response theory, Nat. Phys. **16**, 767 (2020).

[2] H. Shen, B. Zhen, and L. Fu, Topological Band Theory for Non-Hermitian Hamiltonians, Phys. Rev. Lett. **120**, 146402 (2018).

[3] Z. Y. Ge, Y. R. Zhang, T. Liu, S. W. Li, H. Fan, and F. Nori, Topological band theory for non-Hermitian systems from the Dirac equation, Phys. Rev. B **100**, 054105 (2019).

[4] D. Areán, K. Landsteiner, and I. Salazar Landea, Non-Hermitian holography, SciPost Phys. **9**, 032 (2020).

[5] Y. Liu and Y. Wen, Sun Topological hydrodynamic modes and holography, Phys. Rev. D **105**, 086017 (2022).

[6] C. E. Ruter, K. G. Makris, R. El-Ganainy, D. N. Christodoulides, M. Segev, and D. Kip, Observation of parityCtime symmetry in optics, Nat. Phys. **6**, 192 (2010).

[7] A. Regensburger, C. Bersch, M.-A. Miri, G. Onishchukov, D. N. Christodoulides, and U. Peschel, ParityCtime symmetric photonic lattices, Nature (London) **488**, 167 (2012).

[8] R. EI-Ganainy, K. G. Makris, M. Khajavikhan, Z. H. Muslimani, S. Rotter, and N. Christodoulides, Non-Hermitian physics and PT symmetry, Nat. Phys. **14**, 11 (2018).

[9] S. Weimann, M. Kremer, Y. Plotnik, Y. Lumer, S. Nolte, K. G. Makris, M. Segev, M. C. Rechtsman, and A. Szameit, Topologically protected bound states in photonic parityC-time-symmetric crystals, Nat. Mater. **16**, 433 (2017).

[10] C. M. Bender, Making sense of non-Hermitian Hamiltonians, Rep. Prog. Phys. **70**, 947 (2007).

[11] C. M. Bender and S. Boettcher, Real Spectra in Non-Hermitian Hamiltonians having PT Symmetry, Phys. Rev. Lett. **80**, 5243 (1998).

[12] A. Mostafazadeh, Pseudo-Hermiticity versus PT symmetry: The necessary condition for the reality of the spectrum of a non-Hermitian Hamiltonian, J. Math. Phys. (N.Y.) **43**, 205 (2002).

[13] A. Mostafazadeh, Pseudo-Hermiticity versus PT-symmetry. II. A complete characterization of non-Hermitian Hamiltonians with a real spectrum, J. Math. Phys. (N.Y.) **43**, 2814 (2002).

[14] A. Mostafazadeh, Pseudo-Hermiticity versus PT-symmetry III: Equivalence of pseudo-Hermiticity and the presence of antilinear symmetries, J. Math. Phys. (N.Y.) **43**, 3944 (2002).

[15] X. M. Zhao, C. X. Guo, M. L. Yang, Heng-Wang, W. M. Liu, and S. P. Kou, Anomalous non-Abelian statistics for non-Hermitian Majorana zero modes: Alternative approach to universal topological quantum computation, Phys. Rev. B **104**, 214502 (2021).

[16] X. M. Zhao, C. X. Guo, S. P. Kou, Lin-Zhuang, and W. M. Liu, Defective Majorana zero modes in non-Hermitian Kitaev chain, Phys. Rev. B **104**, 205131 (2021).

[17] S. Sachdev and J. Ye, Gapless Spin Fluid Ground State in a Random, Quantum Heisenberg Magnet, Phys. Rev. Lett. **70**, 3339 (1993).

[18] A. Kitaev, A simple model of quantum holography, *Proceedings of the KITP* (2015), http://online.kitp.ucsb.edu/online/entangled15/kitaev/ and http://online.kitp.ucsb.edu/online/entangled15/kitaev2/.

[19] J. Maldacena, D. Stanford, and Z. Yang, Conformal symmetry and its breaking in two dimensional nearly anti–de Sitter space, Prog. Theor. Exp. Phys. **2016**, 12C104 (2016).

[20] P. W. Phillips, L. Yeo, and E. W. Huang, Exact theory for superconductivity in a doped Mott insulator, Nat. Phys. **16**, 1175 (2020).

[21] K. Jensen, Chaos in AdS$_2$ Holography, Phys. Rev. Lett. **117**, 111601 (2016).

[22] J. Maldacena and D. Stanford, Remarks on the Sachdev-Ye-Kitaev model, Phys. Rev. D **94**, 106002 (2016).

[23] S. He and Z. Y. Xian, $T\bar{T}$ deformation on multiquantum mechanics and regenesis, Phys. Rev. D **106**, 046002 (2022).

[24] S. Sachdev, Bekenstein-Hawking Entropy and Strange Metals, Phys. Rev. X **5**, 041025 (2015).

[25] X. H. Ge, S. K. Jian, Y. L. Wang, Z. Y. Xian, and H. Yao, Violation of the viscosity/entropy bound in translationally invariant non-Fermi liquids, Phys. Rev. Res. **2**, 023366 (2020).

[26] W. Cai and X. H. Ge, Superconducting gap ratio from strange metal phase in the absence of quasiparticles, Commun. Theor. Phys. **73**, 025701 (2021).

[27] F. Salvati and A. Tagliacozzo, Superconducting critical temperature in the extended diffusive Sachdev-Ye-Kitaev model, Phys. Rev. Res. **3**, 033117 (2021).

[28] A. Almheiri and J. Polchinski, Models of AdS$_2$ backreaction and holography, J. High Energy Phys. 11 (2015) 014.

[29] J. Engelsoy, T. G. Mertens, and H. Verlinde, An investigation of AdS2 backreaction and holography, J. High Energy Phys. 07 (2016) 139.

[30] J. Maldacena and X. L. Qi, Eternal traversable wormhole, arXiv:1804.00491.

[31] A. Matzkin, Non-Hermitian quantum mechanics: The case of bound state scattering theory, J. Phys. A **39**, 10859 (2006).

[32] S. Sahoo, É. Lantagne-Hurtubise, S. Plugge, and M. Franz, Traversable wormhole and Hawking-Page transition in coupled complex SYK models, Phys. Rev. Res. **2**, 043049 (2020).

[33] W. Cai, X. H. Ge, and G. H. Yang, Diffusion in higher dimensional SYK model with complex fermions, J. High Energy Phys. 01 (2018) 076.

[34] R. A. Davison, W. Fu, A. Georges, Y. Gu, K. Jensen, and S. Sachdev, Thermoelectric transport in disordered metals without quasiparticles: The Sachdev-Ye-Kitaev models and holography, Phys. Rev. B **95**, 155131 (2017).

[35] S. K. Jian and H. Yao, Solvable SYK Models in Higher Dimensions: A New Type of Many-Body Localization Transition, Phys. Rev. Lett. **119**, 206602 (2017).

[36] P. Zhang, More on complex Sachdev-Ye-Kitaev eternal wormholes, J. High Energy Phys. 03 (2021) 087.

[37] P. Gao, D. L. Jafferis, and A. C. Wall, Traversable wormholes via a double trace deformation, J. High Energy Phys. 12 (2017) 151.

[38] S. Cao, Y. C. Rui, and X. H. Ge, Thermodynamic phase structure of complex Sachdev-Ye-Kitaev model and charged black hole in deformed JT gravity, arXiv:2103.16270.

[39] F. Ferrari and F. I. Schaposnik Massolo, Phases of melonic quantum mechanics, Phys. Rev. D **100**, 026007 (2019).

[40] A. M. García-García, J. P. Zheng, and V. Ziogas, Phase diagram of a two-site coupled complex SYK model, Phys. Rev. D **103**, 106023 (2021).